

## Raman frequency shift in oxygen functionalized carbon nanotubes

Z. X. Guo<sup>1</sup>, J. W. Ding<sup>1,2</sup>, Y. Xiao<sup>1</sup>, and D. Y. Xing<sup>2</sup>

<sup>1</sup>*Department of physics, Xiangtan University,  
Xiangtan 411105, Hunan, China*

<sup>2</sup>*National Laboratory of Solid State Microstructures,  
Nanjing University, Nanjing 210093, China  
email: jwding@xtu.edu.cn*

(Dated: October 5, 2018)

In terms of lattice dynamics theory, we study the vibrational properties of the oxygen-functionalized single wall carbon nanotubes (O-SWCNs). Due to the C-O and O-O interactions, many degenerate phonon modes are split and even some new phonon modes are obtained, different from the bare SWCNs. A distinct Raman shift is found in both the radial breathing mode and G modes, depending not only on the tube diameter and chirality but also on oxygen coverage and adsorption configurations. With the oxygen coverage increasing, interesting, a nonmonotonic up- and down-shift is observed in G modes, which is contributed to the competition between the bond expansion and contraction, there coexisting in the functionalized carbon nanotube.

PACS numbers: 63.22.+m; 78.30.-j; 61.46.Fg

Chemical functionalization of carbon nanotubes could offer new and promising avenues to process and assemble tubes, add sensing capabilities, or tune their electronic properties, which are the subject of intensive research.[1, 2] When the functional groups are chemically bonded to the nanotube wall, the tube geometry can be significantly changed. As a result, the C-C force constant and thus the vibrational properties of nanotube will be largely modified. For example, an obvious upshift in the tangential mode vibrations (so-called G modes) was observed experimentally in both single-walled carbon nanotubes (SWCNs) and multi-walled carbon nanotubes (MWCNs) in the acid treatment.[3, 4] For the physically doped nanotubes, such a frequency shift was usually attributed to the variations in the C-C bonds on nanotube, induced by the charge transfer.[5, 6, 7, 8] In the chemically processed nanotubes, however, there exists much stronger interaction between the functional groups and nanotubes, which is of particular importance in the characterization of nanotube-based device. So far, there were few, if any, works reported on how functional groups affect Raman shift in the nanotube. For nanotube-based device applications, this is an outstanding issue and its clarification is greatly desirable.

An oxygen molecule ( $O_2$ ) can be regarded as a simplest kind of functional groups. It was reported that oxygen molecule is very reactive to SWCNs with diameter below 1nm, and the oxidation can even occur at room temperature,[9, 10] forming an oxygen-functionalized SWCN (O-SWCN). Such oxidation can dramatically influence the nanotubes' electrical resistance, thermoelectric power, and local density of states. The Raman shift and even some new vibrational modes may be expected in such an O-SWCN, which may be characterized by Raman spectroscopy. Therefore, the study of the oxygen chemisorption effects on Raman modes can be very helpful to explore the underlying mechanism of the Raman shift in the functionalized nanotubes.

As two types of the most important Raman modes, the radial breathing mode (RBM) and G modes are widely used in the estimation of diameter distribution of nanotubes.[11, 12] To assign the Raman peaks of an O-SWCN, the frequency shift in these modes should be fully taken into account. In addition, an O-SWCN can form several possible configurations, leading to different electronic properties[10], which depend not only on the adsorbed sites and coverage but also on whether the O-O bond breaking or not.[9, 10] It was reported that an SWCN with high adsorbed oxygen has a higher electrical conductance than one with less adsorbed oxygen.[13] How about the influence of the adsorption configurations and coverage on the vibrational properties of an O-SWCN? In the lattice dynamics, it is still an open question and should be further explored.

In this paper, we study the vibrational properties of the O-SWCNs in terms of lattice dynamics theory. Due to the C-O and O-O interactions, many degenerate phonon modes are split and even some new phonon modes are obtained, different from the bare SWCNs. A distinct Raman shift is found in RBM and G modes, depending not only on the tube diameter and chirality but also on oxygen coverage and adsorption configurations. With the oxygen coverage increasing, interesting, a nonmonotonic up- and down-shift is observed in G modes, which is contributed to the competition between the bond expansion and contraction, there coexisting in the functionalized carbon nanotube.

As typical example, we consider the cycloaddition structure for the  $O_2$  adsorption on achiral tube. From previous report, the two configurations,  $O_2$  on top of an axial C-C bond (site TA) and on top of a zigzag C-C bond (site TZ), can lead to chemisorbed structures via cycloaddition (also see Fig. 1), which shall be the focus of present work. To achieve the optimum structure of the O-SWCNs, first-principle plane-wave pseudopotential density functional theory (DFT) is used, performed

in the CASTEP code.[14] For a simplification, we choose a unit cell of about  $4.26\text{\AA}$  to be a supercell in zigzag tube, while two unit cell of about  $4.92\text{\AA}$  in armchair tube.[15] The validity of the optimum results has been confirmed by using even larger supercell.

Fig. 1 shows the optimized geometries of a (10,0) O-SWCN in both TA and TZ configurations, which are similar with the previous results.[9, 10] Interestingly, both the expansion and contraction of the C-C bonds are obtained in the O-SWCN, different from the physically doped SWCNs only with a bond expansion or contraction. In TA configuration, for example, three C-C bonds at the adsorbed site are markedly expanded to be 1.500, 1.498 and  $1.521\text{\AA}$ , respectively, while the bonds near the adsorbed site is contracted, there appearing a minimal length of about  $1.374\text{\AA}$ , shorter than  $1.417\text{\AA}$  of the bare tube. Far from the adsorbed site, little change in the C-C bonds is observed, almost not affected by the oxidation. The bond expansion can be understood by the fact that a strong C-O covalent bond has been formed by the introduction of holes into the  $\pi^*$  orbital,[7] forming a  $sp^3$ -like rehybridization at the adsorbed site. This leads to the bond length increasing, different from the  $\text{Br}_2$  donor graphite intercalation compounds, in which the C-C bonds still keep  $sp^2$  hybridization. As for the bond contraction, it is mainly contributed to the charge transfer from SWCN to oxygen,[5, 6, 7, 8] similar to that in the physically doped SWCNs, where the gain (removal) of electrons induces the C-C bond expansion (contraction) and thus resulting in a downshift (upshift) in G modes.[7, 8] The coexistence of the bond expansion and contraction may indicate a new mechanism of Raman shift in the functionalized SWCNs.

For the lattice dynamic calculations, the vibrations of the carbon atoms on the nanotube can be modeled by the force constant model in terms of the force constants of graphene, up to the fourth next neighboring interaction.[16] To incorporate the oxygen adsorption effects, the C-C force constants have been corrected through the distorted bond lengths obtained above.[17, 18] As for the C-O and O-O bond interactions, we use the well-known Tersoff-Brenner bond order potential,[19] and the potential parameters in Ref.20. Shown in Fig. 2 are the phonon dispersions of the (10,0) bared SWCN and O-SWCN in TA configuration. For the O-SWCN, there are three acoustic phonon modes at around  $\Gamma$  point: two transverse, one longitudinal, similar with the bared SWCN. However, the twisting mode has a non-zero frequency of about  $20\text{cm}^{-1}$  at the center of Brillouin zone, different from the bared SWCN, which is attributed to the tube geometry distortion and the oxygen vibrational interaction. Due to the tube symmetry destruction, interestingly, many doubly degenerate phonon modes are split. For example, the lowest  $E_{2g}$  mode is split into two absolute subbands at  $58\text{cm}^{-1}$  and  $68\text{cm}^{-1}$ , shifted from  $62\text{cm}^{-1}$  of the bared SWCN. Such splitting will have an important influence on the low-temperature specific heat.[21] Also, some new phonon modes appear below

$300\text{cm}^{-1}$  with nearly linear dispersion, which can be contributed to the O-O bond stretching vibrations and the coupling vibrations between the oxygen and the tube. Moreover, the highest frequency mode of  $1607\text{cm}^{-1}$  is newly obtained at  $\Gamma$  point, higher than  $1600\text{cm}^{-1}$  of the bare tube, which is ascribed to the strong C-O stretching vibrations. Similar results are also obtained in TZ configuration. The splitting of Raman modes and the new vibrational modes are expected to be observed by Raman spectroscopic experiment.

Also shown in Table 1 are the RBM and G mode frequencies of the (10,0) O-SWCN in both TA and TZ configurations. For the bare (10,0) tube, the RBM frequency is obtained to be of  $294\text{cm}^{-1}$ , in good agreement with the experiment and the first principle results.[25, 26] In the TA (TZ) configuration of the O-SWCN, the RBM frequency downshifts to be  $278\text{cm}^{-1}$  ( $276\text{cm}^{-1}$ ), decreased by  $16(18)\text{cm}^{-1}$ , while the upshifts are obtained in the G modes, increasing by  $8(4)\text{cm}^{-1}$  in  $E_{1g}$ ,  $6(13)\text{cm}^{-1}$  in  $A_{1g}$ , and  $7(3)\text{cm}^{-1}$  in  $E_{2g}$ , respectively. It is shown that the frequency shift in both RBM and G modes depends strongly on the adsorption configurations, which should be considered in the nanotube characterization by the Raman spectroscopic experiment.

To explore the dependence of the Raman shift on the tube diameter and chirality, we calculate the RBM of armchair (5,5) and zigzag (8,0) O-SWCNs, which have the similar tube diameter. For the (5,5) O-SWCN, the O-O bond direction is perpendicular to the tube axis. In the case of the (8,0) O-SWCN, the TA configuration is considered. For the bare and oxygenated (8,0) SWCNs, the RBM frequencies are obtained to be  $359\text{cm}^{-1}$  and  $329\text{cm}^{-1}$ , respectively. The frequency shift in RBM,  $\Delta\omega = -30\text{cm}^{-1}$  is much larger than that of (10,0) O-SWCN. This indicates the dependence of the Raman shift on tube diameter, *i.e.*, the larger the frequency shift, the smaller the tube diameter. In the (5,5) O-SWCN, on the other hand, the RBM frequency of about  $272\text{cm}^{-1}$  shifts from  $336\text{cm}^{-1}$  of the bare (5,5) tube. The frequency shift ( $\Delta\omega = -64\text{cm}^{-1}$ ) is larger than two times that of the (8,0) O-SWCNs. At a given tube diameter, obviously, an armchair tube is more sensitive to the oxidation than a zigzag one, showing up a chirality-dependence of the Raman shift. The results give a possibility to determine the tube diameter and chirality of the O-SWCNs by Raman spectroscopic experiment.

Now we further study the dependence of Raman shift on the coverage (defined by O/C ratio  $x$ ). As a typical example, Fig.3 shows the frequency of  $E_{1g}$  mode (one of G modes) in the (10,0) O-SWCN with TA configuration as a function of  $x$ . For a given  $x$ , there may be much many configurations. To obtain the qualitative relation between Raman shift and the coverage, the oxygen atoms are simply considered to be averagely adsorbed as possible, especially for a large  $x$ . From Fig. 3,  $E_{1g}$  mode first upshifts and then downshifts with  $x$  increasing. There exists a maximum of  $1611\text{cm}^{-1}$  at  $x = 0.25$ , showing a nonmonotonic behavior of the frequency shift. At half

coverage ( $x = 0.5$ ), it even downshifts to be  $1580\text{cm}^{-1}$ , lower than  $1585\text{cm}^{-1}$  of the bare SWCN. For other G modes, the frequency shift in both  $A_{1g}$  and  $E_{2g}$  is also calculated, which has the similar dependence on coverage to that in  $E_{1g}$ . In order to explore the origin of the G mode shift, we remove the C-O vibrational interactions and recalculate the  $E_{1g}$  mode in terms of the same optimum geometry above. As a result, the frequencies are overall downshifted, lower than those in the presence of the C-O vibrational interactions, as shown in Fig. 3. Therefore, it is shown that there exists a large contribution of the C-O vibration to the upshift in G modes.

In the absence of the C-O vibrational interactions, also, the nonmonotonic behavior is still obtained for the frequency shift in  $E_{1g}$  modes. This may be due to the competition between the rehybridization induced bond expansion in the bonds at the adsorbed sites and the charge transfer induced bond contraction in the bonds near the adsorbed site. At low coverage, the bond contraction effect is dominant, leading to the upshift in G modes, while the bond expansion effect would become predominant at high coverage, resulting in an decrease of G mode frequency with  $x$ . Therefore, there may exist a new competition mechanism between the bond expansion and contraction, coexisting in the functionalized nanotube, different from the physically doped SWCNs.[7, 22] In some alkali-metal doped nanotube bundles, the similar changes in G modes with the coverage had been experimentally observed via vapor phase doping or redox reaction.[23, 24] Consequently, our results can contribute to the understanding of the origin of the G mode shift in the functionalized carbon nanotube. In the case of neglecting the C-O vibrational interactions, in addition, there exists a locally minimal frequency of  $E_{1g}$  mode at

$x = 0.1$ . In this case, the O-SWCN is considered to have its highest symmetry of mirror symmetry. To understand this local minimum, we recalculate the  $E_{1g}$  mode at the same coverage but an asymmetrical configuration. The obtained frequency of  $1592\text{cm}^{-1}$  is higher than  $1586\text{cm}^{-1}$  in the symmetrical case, which further shows the dependence of Raman shift on the configurations.

In summary, the vibrational properties of oxygen functionalized nanotubes are studied in terms of lattice dynamics theory. Due to the C-O and O-O vibrational interactions, many degenerate phonon modes are split and even some new phonon modes are obtained, which can be observed in the Raman spectroscopic experiment. Also, the Raman shift is observed in the O-SWCNs, depending not only on the tube diameter and chirality but also on oxygen coverage and adsorption configurations. It is found that the bond expansion and contraction coexist in the functionalized carbon nanotube. With the coverage increasing, a nonmonotonic behavior of the G mode shift is obtained, which is contributed to the competition between the bond expansion and contraction. The results can be helpful to the characterization and practical application of functionalized carbon nanotube-based device.

**Acknowledgments:** This work was supported by National Natural Science Foundation of China (Nos.: 10674113 and 10374046), Hunan Provincial Natural Science Foundation of China (No.: 06JJ5006), and partially by Scientific Research Fund of Hunan Provincial Education Department (No.: 06A071).

- 
- [1] C. A. Dyke and J. M. Tour, *J. Phys. Chem. A* 108, 11151 (2004).
  - [2] X. Lu and Z. Chen, *Chem. Rev.* 105, 3643 (2005).
  - [3] U. J. Kim, C. A. Furtado, X. Liu, G. Chen, and P. C. Eklund, *J. Am. Chem. Soc.* 127, 15437 (2005).
  - [4] H. Murphy, P. Papakonstantinou, and T. I. T Okpalugo, *J. Vac. Sci. Technol. B* 24, 1071 (2006).
  - [5] R. A. Jishi and M. S. Dresselhaus, *Phys. Rev. B* 45, 6914 (1992).
  - [6] C. T. Chan, W. A. Kamitakahara, K. M. Ho, and P. C. Eklund, *Phys. Rev. Lett.* 58, 1528 (1987).
  - [7] A. M. Rao, P. C. Eklund, S. Bandow, A. Thess, and R. E. Smalley, *Nature (London)* 388, 257 (1997).
  - [8] B. Akdim, X. Duan, D. A. Shiffler, and R. Pachter, *Phys. Rev. B* 72, 121402(R) (2005).
  - [9] S. P. Chan, G. Chen, X. G. Gong, and Z. F. Liu, *Phys. Rev. Lett.* 90, 086403 (2003).
  - [10] Y. F. Zhang, and Z. F. Liu, *J. Phys. Chem. B* 108, 11435 (2004).
  - [11] S. Bandow, S. Asaka, Y. Saito, A. M. Rao, L. Grigorian, E. Richter, and P. C. Eklund, *Phys. Rev. Lett.* 80, 3779 (1998).
  - [12] M. Milnera, J. Kurti, M. Hulman, and H. Kuzmany, *Phys. Rev. Lett.* 84, 1324 (2000).
  - [13] Philip G. Collins, Keith Bradley, Masa Ishigami, and A. Zettl, *Science* 287, 1801 (2000).
  - [14] M. D. Segall, P. L. D. Lindan, M. J. Probert, C. J. Pickard, P. J. Hasnip, S. J. Clark, and M. C. Payne, *J. Phys.: Condens. Matter* 14, 2717 (2002).
  - [15] H. J. Liu, C. T. Chan, Z. Y. Liu, and J. Shi, *Phys. Rev. B* 72, 075437 (2005).
  - [16] R. Saito, G. Dresselhaus, and M. S. Dresselhaus, *Physical Properties of Carbon Nanotubes* (Imperial College Press, London, 1998).
  - [17] Y. Xiao, Z. M. Li, X. H. Yan, Y. Zhang, Y. L. Mao, and Y. R. Yang, *Phys. Rev. B* 71, 233405 (2005).
  - [18] Z. X. Guo, J. W. Ding, Y. Xiao, and Y. L. Mao, *J. Phys. Chem. B*, 110, 21803 (2006).
  - [19] D. W. Brenner, *Phys. Rev. B* 42, 9458 (1990).
  - [20] Y. Yamaguchi, and J. Gspann, *Phys. Rev. B* 66, 155408 (2002).
  - [21] V. N. Popov, *Phys. Rev. B* 66, 153408 (2002).
  - [22] G. U. Sumanasekera, J. L. Allen, S. L. Fang, A. L. Loper, A. M. Rao, and P. C. Eklund, *J. Phys. Chem. B* 103, 4292

- (1999).
- [23] N. Bendiab, E. Anglaret, J. L. Bantignies, A. Zahab, J. L. Sauvajol, P. Petit C. Mathis and S. Lefrant, Phys. Rev. B 64, 245424 (2001).
- [24] G. Chen, C. A. Furtado, S. Bandow, S. Iijima, and P. C. Eklund, Phys. Rev. B 71, 045408 (2005); G. Chen, C. A. Furtado, U. J. Kim, and P. C. Eklund, Phys. Rev. B 72, 155406 (2005).
- [25] H. M. Lawler, D. Areshkin, J. W. Mintmire, and C. T. White, Phys. Rev. B 72, 233403 (2005).
- [26] J. Maultzsch, H. Telg, S. Reich, and C. Thomsen, Phys. Rev. B 72, 205438 (2005).

Table. 1. Frequencies of RBM and G modes of the bare (10,0) SWCN and O-SWCN in both TA and TZ configurations (in units of  $\text{cm}^{-1}$ ).

Figure. 1. Optimized structures of (10,0) O-SWCNs in (a) TA and (b) TZ configurations.

Figure. 2. Phonon dispersion relations of the (10,0) SWCN (a) and O-SWCN in TA configuration (b).

Figure. 3.  $E_{1g}$  mode frequency of the (10,0) O-SWNT in TA configuration as a function of the coverage  $x$  in both the absence and the presence of the C-O vibrational interactions.

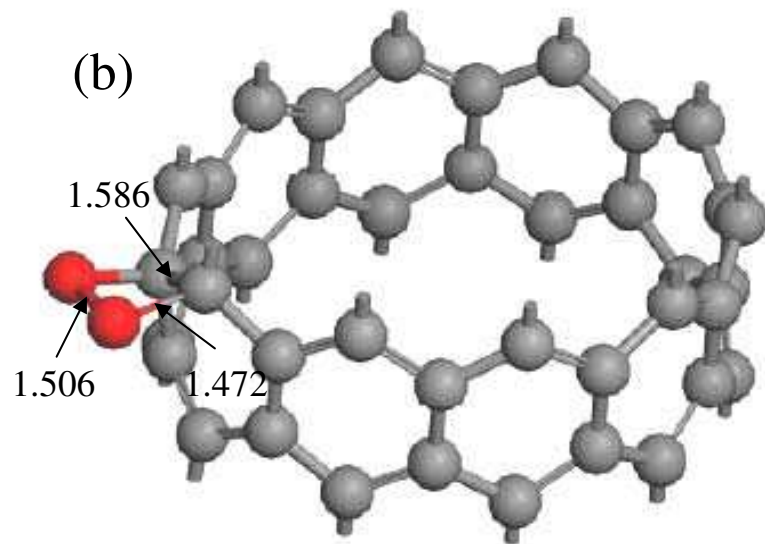
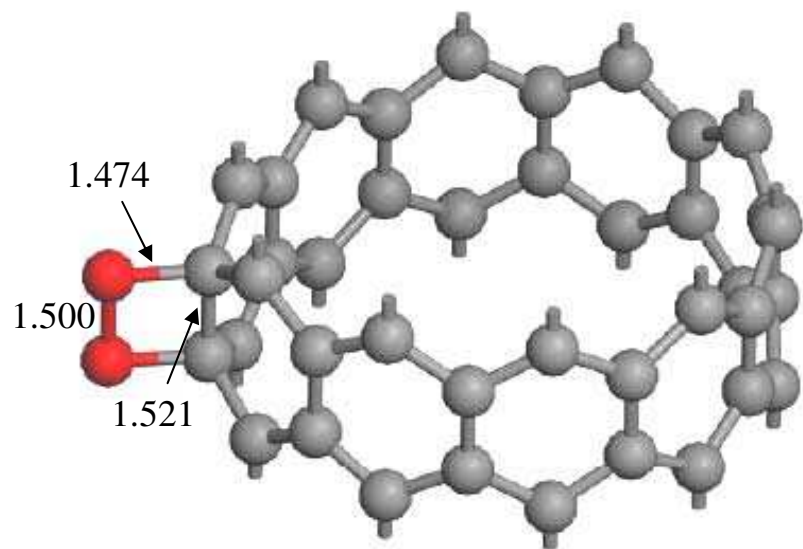


FIG. 1

Table. 1. Frequencies of RBM and G modes of the bare (10,0) SWCN and O-SWCN in both TA and TZ configurations (in units of  $\text{cm}^{-1}$ ).

	RBM	G Modes		
		$E_{1g}$	$A_{1g}$	$E_{2g}$
SWCN	294	1585	1566	1535
Site TA	278	1592	1572	1543
Site TZ	276	1588	1579	1539

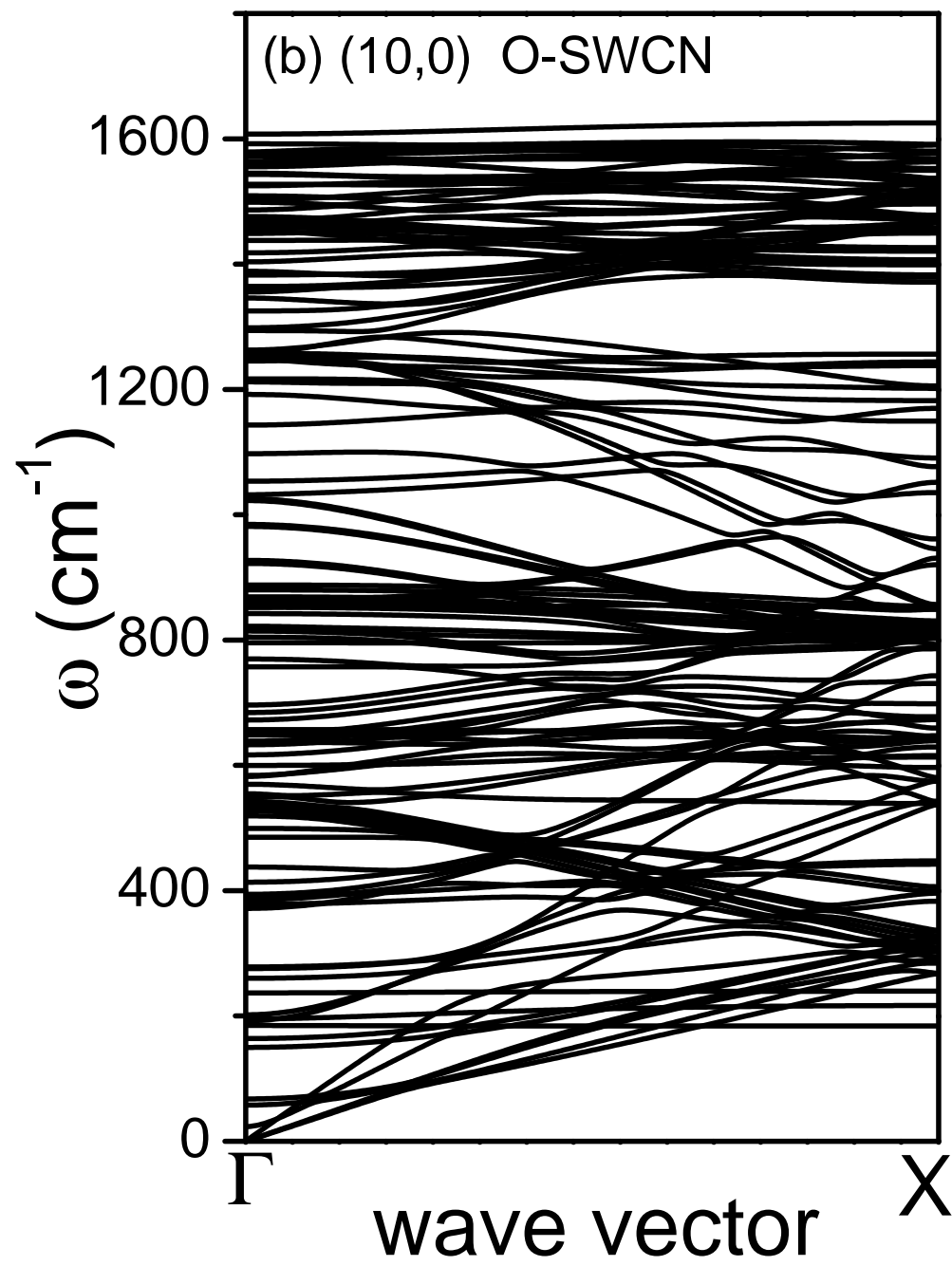
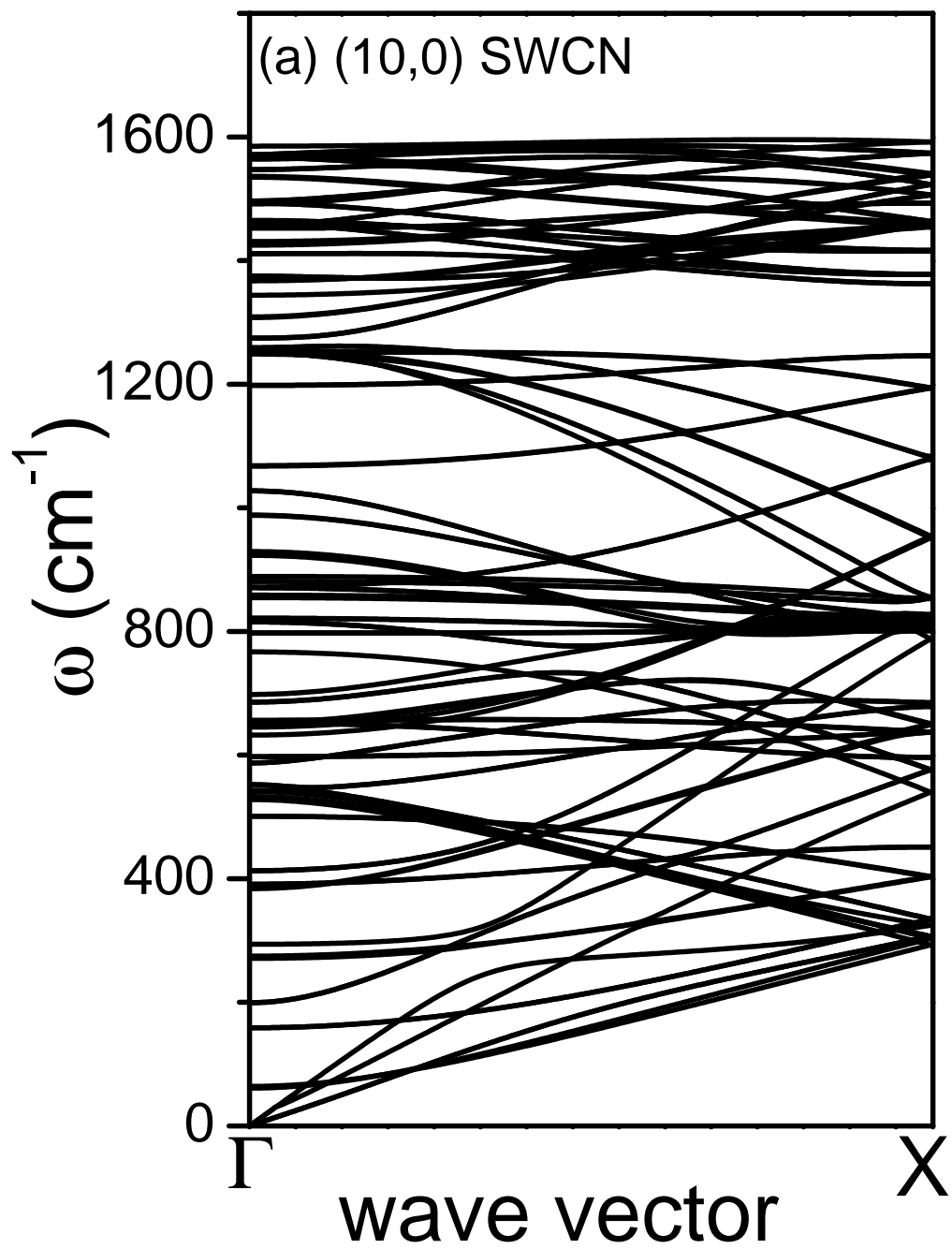


FIG. 2

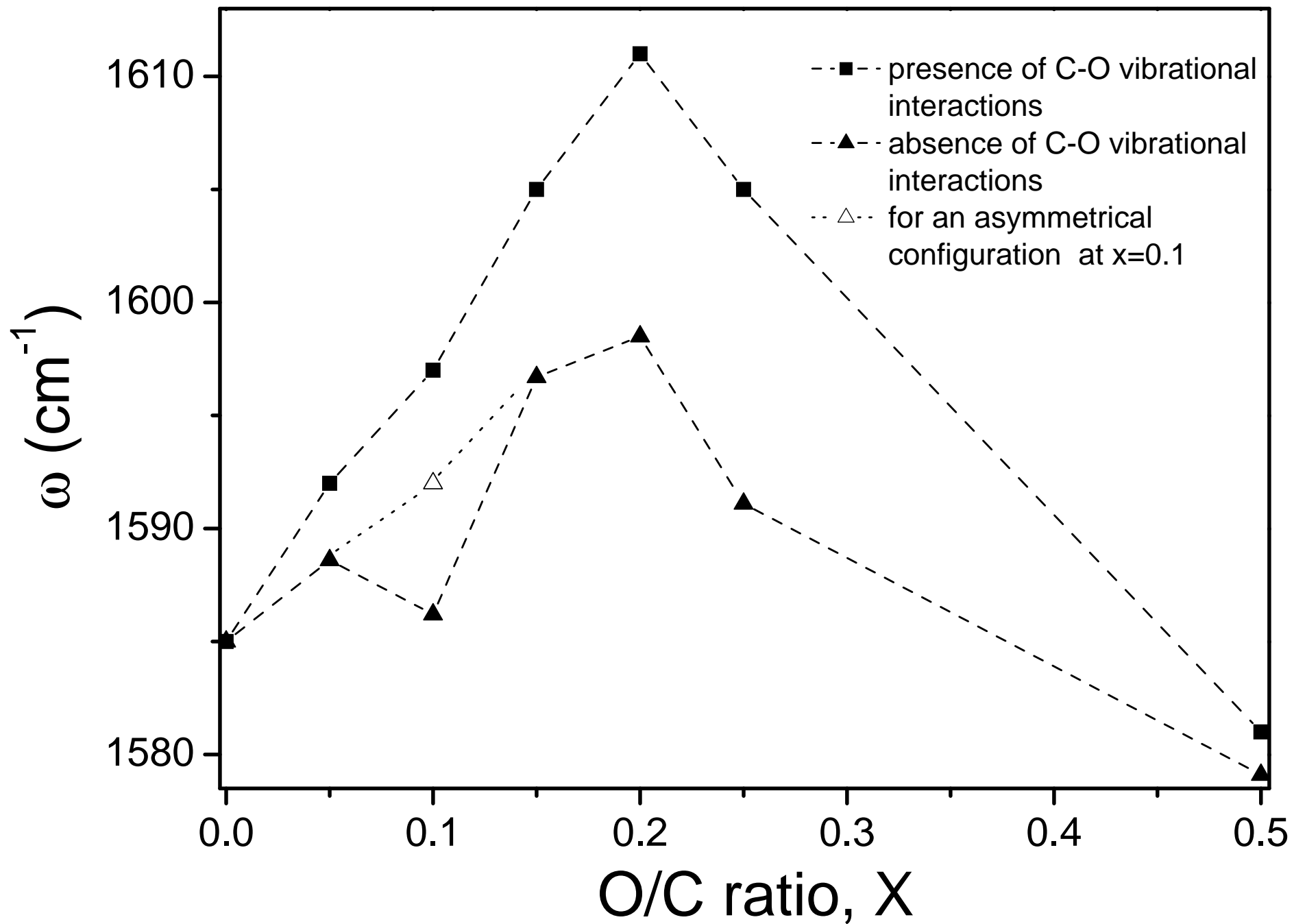


FIG. 3